ELSEVIER

Biochimica et Biophysica Acta 1185 (1994) 221–227

BBA Biochimica et Biophysica Acta

Measurement of unidirectional $P_i \rightarrow ATP$ flux in lamb myocardium in vivo

Michael A. Portman *

Division of Cardiology, Department of Pediatrics / RD20, University of Washington School of Medicine, Seattle, WA 98195, USA

(Received 15 July 1993)

Abstract

Unidirectional myocardial ATP synthesis, $P_i \rightarrow ATP$ flux, was studied in vivo using ^{31}P magnetization transfer techniques in intact sheep hearts ($n = 5$) which were functioning aerobically. Myocardial oxygen consumption (MVO) expressed as μmoles of oxygen atoms/gm/min was estimated using linear regression analysis of data derived from sheep ($n = 23$), which had undergone continuous MVO measurement during graded stepups in epinephrine induced work loads. During the saturation transfer experiment, epinephrine, beginning at 1 μg/kg per min was infused to achieve a higher steady-state work load and level of MVO. The unidirectional $P_i \rightarrow ATP$ flux was found to increase significantly ($P < 0.05$) during increases in rate pressure product and MVO. These data show that the unidirectional $P_i \rightarrow ATP$ flux is at least 3-times higher than the peak ATP synthesis rate, achieved through oxidative phosphorylation in these experiments, and more than a magnitude higher than the peak ATP synthesis rate through glycolysis. Therefore, forward $P_i \rightarrow ATP$ flux through glycolysis is the major contributor to the measured $P_i \rightarrow ATP$ flux and these ATP producing bidirectional glycolytic reactions are in a near equilibrium state. Furthermore, $\Delta P_i \rightarrow ATP/\Delta MVO$, 2.70 ± 0.29 (S.E.) elicited during epinephrine infusion is similar to classically derived P:O values, indicating that most of the change in unidirectional flux is due to oxidative phosphorylation and that minimal disturbance in the glycolytic near equilibrium occurs under these conditions.

Key words: Oxidative phosphorylation; Phosphate-ATP flux; Glycolysis; ATP; NMR, ^{31}P-; Saturation transfer; (Sheep myocardium)

1. Introduction

Cellular ATP synthesis occurs predominantly through oxidative phosphorylation in aerobic myocardium, although an additional contribution occurs through the ATP producing reactions of glycolysis [1,2]. Specific enzymes involved in glycolytic ATP synthesis have been noted to catalyze their reactions at high rates bidirectionally [1–3], although most studies related to glycolytic control through these enzymes have examined net rates [4–7]. Recent ^{31}P magnetic resonance studies of perfused hearts [1,2] and postischemic myocardium in vivo [8] employing saturation transfer techniques have indicated that these glycolytic reactions occur near equilibrium. Measurement of the unidirectional ATP synthesis rate, referred to as $P_i \rightarrow ATP$ flux throughout this paper, in myocardium in vivo has been hampered by the complexities involved with the magnetic resonance techniques and the inability to obtain the adequate resolution and signal to noise required for the experiment [8]. Therefore, the proportion of $P_i \rightarrow ATP$ flux contributed through glycolysis remains unknown in normal myocardium in vivo. The purpose of this study was to measure this glycolytic contribution, $_{gly}P_i \rightarrow ATP$ flux, and determine whether these reactions function near equilibrium in myocardium in vivo, which has not been subjected to ischemia.

2. Methods

Animal preparation. Mixed breed lambs (age 14–21 days; $n = 5$), weighing between 8 and 12 kg, were sedated with an intramuscular injection of 10 mg/kg

* Corresponding author. Fax: +1 (206) 5433184.

SSDI 0005-2728(93)E0223-D

ketamine and 0.2–0.4 mg/kg xylazine, intubated, and then ventilated (model D-900 pediatric ventilator, Siemens-Elema, Schaumberg, IL) with an anesthesia mixture of 0.5–1.0% halothane and 99% oxygen. Femoral arterial cannulation was performed for monitoring systemic blood pressure and sampling blood. Arterial pH was maintained between 7.35 and 7.45 by adjustment of ventilatory tidal volume and correction of metabolic acidosis with sodium bicarbonate. Following a median sternotomy, the pericardial fat pad was exposed and removed. Platinum-tipped pacing electrodes were sutured to the right atrial appendage. A 3 cm diameter single-turn NMR surface coil was sutured to the pericardium overlying the left ventricle. This coil placement allowed unrestricted cardiac movement and filling, while keeping the coil in reproducible proximity of the heart. The thoracotomy opening was then sealed with plastic wrap to prevent water loss. The sheep was wrapped in a water circulating heating blanket to maintain body core temperature at 38°C, and placed in a lucite cradle which slid into the spectrometer. The surface coil was positioned at or near the magnetic center of the system.

NMR measurements. Following transfer of the lamb into the magnet, the NMR surface coil was tuned to 81 MHz and matched to 50 Ω using a network analyzer with a connecting cable calibrated for use within the magnet field. Respiration was maintained within the magnet via 15 feet of tubing attached to the expiratory and inspiratory ports of the ventilator. Blood pressure was monitored using a solid state nonmagnetic pressure transducer (Cobe Lab., Lakewood, CO) positioned just outside the magnet bore.

NMR data were collected with a 4.7 Tesla, 26 cm clear bore spectrometer employing OMEGA (General Electric, Fremount CA) software. Shimming on the ^{1}H free induction decay at 200 MHz and acquisition of ^{31}P spectra were collected at 81 MHz as previously described [9], using both cardiac and respiratory gating. The proton linewidth was determined prior to performance of ^{31}P spectroscopy. Experiments were performed only if a proton linewidth less than 40 Hz was obtained.

Saturation transfer experiments were conducted to determine the $P_i \rightarrow$ ATP flux. Saturation was achieved by selectively irradiating the γ phosphate peak of the ATP resonance for 5 s with a decoupler at low power utilizing a separate radiofrequency channel and observing the effect on the P_i peak magnitude. The control for this experiment was a 5 s irradiation of the region equidistant for P_i but on the higher frequency side. Control acquisitions were interleaved with experimental. In this experiment, acquisition time was approximately 0.41 s. The cardiac and respiratory gating sequence triggered the spectrometer every 6 s.

The unidirectional pseudo-first-order forward rate constant, K_f, was determined using the following equation: $K_f = (1/\tau) \cdot (1 - M_s/M_o)$, where M_s is the magnetization of P_i with saturation, and M_o is the P_i magnetization obtained during the control [10]. τ is the spin lattice relaxation time obtained during a burst saturation recovery experiment with selective saturation for 5 s on γ ATP using a decoupler on an alternate radiofrequency channel. Burst saturation recovery was accomplished using the following sequence $60 \times$ (400 μs pulse, 1 ms delay); variable delay; 40–50 μs read pulse and acquisition [11,12]. The 5 s of selective excitation always preceded and ended at the read pulse. Variable delays of 5 s, 3 s, 1 s, 0.5 s and 0.05 s were used and 120 acquisitions were averaged from each. Generated data were analyzed using an exponential line fitting program for determination of τ values.

All spectra were acquired using 2K data points with an acquisition time of 410 ms. Prior to Fourier transformation 5 Hz linebroadening was applied as the only processing. All NMR peak areas were determined using a peak deconvolution program as previously described [13]. All phosphorous spectra were referenced to PCr for chemical shift. P_i concentration was estimated from the P_i/ATP ratio assuming an intracellular ATP concentration of 6.9 μmol/g wet weight corrected for intracellular water content from previously reported values in sheep [9] myocardium. This value is similar to those reported by Ingwall et al. [14], 6.0 ± 0.3 in newborn and 6.1 ± 0.4 in adult sheep myocardium. $P_i \rightarrow$ ATP was calculated as $K_f[P_i]$.

Saturation correction. In order to increase the number of acquisitions performed and hence improve P_i peak signal to noise ratio without increasing the length of the experiment, a 6 s interpulse delay was utilized in these studies. Using previously published T_1 values in the sheep heart [9] for P_i ($T_1 = 2.5 \pm 0.3$ s) and β ATP ($T_1 = 1.5 \pm 0.1$ s) a saturation correction factor can be calculated from:

$$\left[(1 - e^{-t/T1})_{ATP}\right] / \left[(1 - e^{-t/T1})_{P_i}\right]$$

where t is the delay between 90° read pulses and T_1 are the above values for each resonance. P_i/ATP for all experiments was multiplied by this factor (1.08) to correct for saturation of the P_i resonance. This factor was also verified by comparing P_i/ATP obtained in a simple one pulse experiment using a 6 s interpulse delay with fully relaxed P_i/ATP (16 s interpulse delay) obtained using the same pulse sequence in the five sheep from the present study (correction factor = 1.06 $\pm$ 0.03). These above calculations all assume a perfect 90° pulse for simplicity; however, due to inhomogeneities inherent in a surface coil, different parts of the sample will experience a range of flip angles either greater or less than 90°. This inhomogeneity can introduce some error into these calculations. P_i M_s/M_0 was also corrected for saturation (multiplying M_0 by 1.08),

as M_0 is affected by saturation but M_s is not due to a τ which is less than 20% of the interpulse delay.

Protocol. Initially, saturation transfer and τ determinations were performed at a baseline work load. Cardiac pacing which enhanced shimming through accurate gating was performed at the lowest harmonic of the respiratory rate (30/min) above the intrinsic heart rate, usually 150 beats per min. The burst saturation recovery experiment, which usually took 1 to 1.5 h to complete, was followed by eighty magnetization transfer experimental acquisitions interleaved with an equal number of control acquisitions as described above. After completion of baseline studies, an intravenous epinephrine infusion was begun at 1 μg/kg per min and slowly increased until a doubling of mean rate-pressure product was obtained. The final dose was usually near 3 μg/kg per min. Pacing was continued but the rate increased if the epinephrine induced rate exceeded the paced rate. Epinephrine was titrated to maintain a stable systemic blood pressure. Magnetization transfer experimental and control acquisitions were obtained followed by the burst saturations recovery τ experiment. Arterial systolic, diastolic and mean blood pressures were recorded throughout, and arterial blood gases monitored every 12 min.

Estimation of myocardial oxygen consumption. Because of the prolonged nature of these experiments, on line measurement of myocardial oxygen consumption was not performed. However, separate experiments were done in order to establish the relationship between myocardial oxygen consumption and mean rate-pressure product in this animal model, while using a similar epinephrine infusion. These experiments utilized on line flow measurement in a coronary sinus shunt. The details of this procedure are described elsewhere [9,12]. Sheep, age 14–70 days, $n = 23$; underwent graded step-ups in epinephrine infusion as previously described [12] under conditions similar to those in the present study. The relationship between rate-pressure product and myocardial oxygen consumption was determined using linear regression analysis and is MVO = 0.64 + 0.46RPP, (slope S.E. = $\pm$0.02; $R = 0.82$). Myocardial oxygen consumption rates (μmol of oxygen atoms/g per min) in the $P_i \rightarrow$ ATP flux experiments were estimated using the results of this linear regression analysis. A similar study was performed using newborn sheep, age 3–10 days ($n = 14$). The relationship between these parameters, MVO = 0.68 + 0.46RPP (slope S.E. = $\pm$0.04; $R = 0.79$) is similar to that in older sheep indicating that there is minimal age related difference in the relation between myocardial oxygen consumption and rate-pressure product in this animal model.

Data analysis. NMR and physiologic parameters obtained from the low work load state were compared with high work load state using a paired t-test. Statistical significance was defined as $P < 0.05$, and all data noted as mean $\pm$ S.E.

3. Results

Performance of this experiment is limited by the achievement of adequate resolution and P_i peak signal to noise. This, however, was most dependent on adequate shimming. A proton linewidth less than 40 Hz was obtained in five experiments. In these experiments therefore, necessary signal to noise and resolution were obtained in order to measure $P_i \rightarrow$ ATP flux. This is demonstrated in Figs. 1 and 2, which show sample spectra from these experiments. Fig. 1 demonstrates the frequency of selective excitation in spectra A and B, denoted by arrows. Note that there is total eradication of the γ-ATP peak denoted by the arrow in spectra B. The total obliteration of this peak demonstrates the adequacy of the saturating pulse, even though there is some inhomogeneity of the radiofrequency field profile generated by the surface coil. In Fig. 1 C, the difference spectrum (A–B), the arrow denotes the difference in P_i, which is due to saturation transfer from ATP. The location of this difference at 4.9 ppm indicates that there is signal loss due to saturation of the P_i peak. Difference spectra were obtained for each work state in all animals to ascertain the identification of the intracellular phosphate peak. Magnetization transfer also occurs to the phosphocreatine peak, as well as to the α and β ATP peaks. This phenomenon has been previously reported [11,12] and

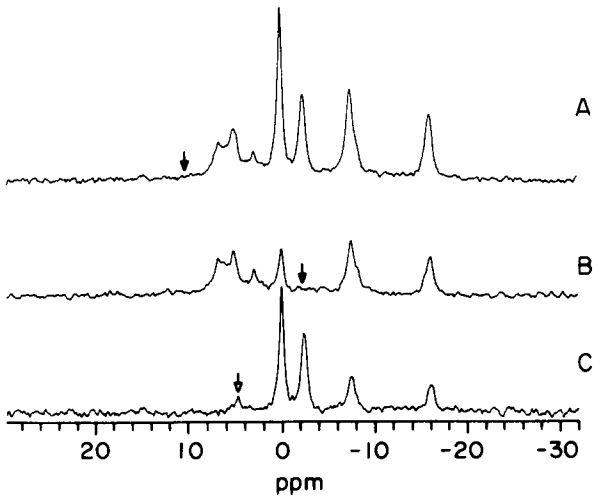

Fig. 1. (A) represents control spectrum (80 acquisitions) during a saturation transfer experiment with arrow denoting the decoupler frequency. Reference peak at 0 ppm is phosphocreatine. (B) illustrates the spectrum obtained with selective irradiation at the γ-ATP frequency (arrow). (C) represents the difference spectrum ((A)–(B)). The arrow marks the difference in P_i signal at 4.9 ppm. These spectra were obtained at the low work load state.

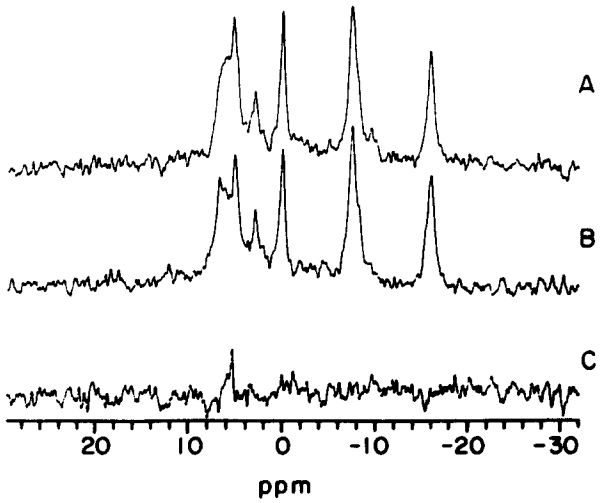

Fig. 2. (A) and (B) illustrate spectra where selective irradiation occurs at γ-ATP. Signal to noise ratio is reduced compared to Fig. 1A, but comparable to Fig. 1B. Signal is reduced because of saturation transfer which reduces the intensity of the phosphocreatine peak. Conditions in (A) are at low work load. (B) illustrates a spectrum using the same pulse sequence in the same animal, but during a higher work load due to epinephrine infusion. (C) represents the difference spectrum. Note that there are no changes in PCr or ATP, but a difference in P_i peak area occurs at approx. 5.0 ppm.

is not due to broadband saturation as evidenced by the fact that no saturation of the phosphomonester resonances occurs. Fig. 2 demonstrates the effect of increasing work load on magnetization transfer to P_i. A and B illustrate spectra, where selective irradiation occurs at γ-ATP. Conditions are at low work load. B illustrates a spectrum using the same pulse sequence in the same animal, but during a higher work load due to epinephrine infusion. C represents the difference spectrum. Note, that there are no changes in PCr or ATP. However, there is a difference in P_i peak area at 5.0 ppm. P_i peak area, and thus P_i concentration did not change in the control irradiation spectra between the two work states. Therefore, this difference spectrum probably illustrates a decrease in P_i signal due to an increase in magnetization transfer at the higher work load. Fig. 3 shows a typical exponential curve fitting generated from the P_i peak areas obtained using the burst saturation recovery sequence, τ in this case equals 0.802 s.

Phosphorus metabolites and pH

Table 1 summarizes the data from these experiments and provides the result of the paired t tests between the two work states. In these juvenile sheep, high myocardial intracellular phosphate concentrations are similar to previous findings in younger newborn sheep [13], but the stability of myocardial intracellular phosphates during work increases resembles the situation in more mature sheep [9,12]. There was no significant change in PCr or β ATP peak area between the

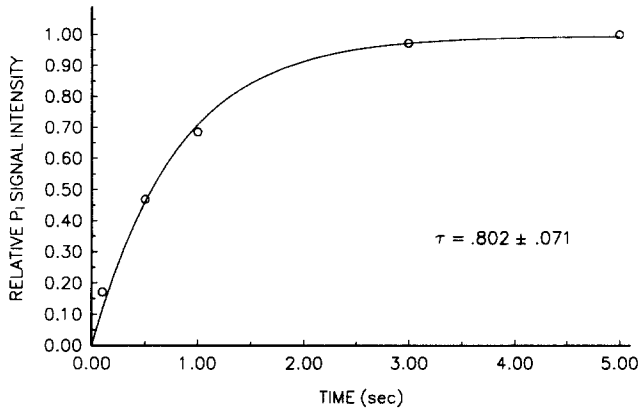

Fig. 3. This plot shows the exponential fitting curve resulting from P_i peak areas obtained from the burst saturation recovery to determine the apparent relaxation constant (τ) of the P_i resonance peak.

two work states, when initial area was compared to the area obtained at high work load. Intracellular pH was determined from the chemical shift of the intracellular P_i peak referenced to PCr as previously described [9,13,15] using a calibration curve equation: $pH = 6.68 + \log(\delta - 3.25)/(5.7 - \delta)$ [16]. There was no significant change in baseline pH 7.11 ± 0.02 when compared to high work load pH 7.10 ± 0.03.

Hemodynamic parameters

Large increases in rate-pressure rate product were achieved in each individual experiment. Calculation of myocardial oxygen consumption from the linear regression data reveals that greater than a 2-fold average increase was achieved during the transition from low to

Table 1
Saturation transfer and hemodynamic parameters ($n = 5$)

Work load	Low	High	t
P_i (μmol/g)	2.76 ± 0.41	2.60 ± 0.41	n.s.
M_s/M_o	0.56 ± 0.09	0.43 ± 0.10	$P < 0.05$
τ(s)	0.91 ± 0.02	0.92 ± 0.07	n.s.
K_f (s^{-1})	0.49 ± 0.09	0.62 ± 0.16	$P = 0.054$
Flux	81 ± 14	97 ± 16	$P < 0.05$
RPP	10070 ± 1513	23505 ± 3357	$P < 0.005$
MVO	5.32 ± 0.72	11.36 ± 1.64	$P < 0.005$
pH	7.11 ± 0.02	7.10 ± 0.03	$P < 0.05$

Data represent parameters obtained from a low work load state, and an epinephrine induced high work load state. Values are means ± S.E.: n = number of experimental animals; P_i is intracellular phosphate concentration, M_s/M_o is the ratio of P_i peak area during saturation of γ ATP to the peak area during a control period. τ is the apparent relaxation time of P_i determined during burst saturation recovery experiment with simultaneous selective saturation of γ ATP. K_f is the unidirectional pseudo first order forward ($P_i \rightarrow$ ATP) rate constant and is calculated from $K_f = (1/\tau)\cdot(1 - M_s/M_o)$. Flux is the reaction rate of $P_i \rightarrow$ ATP in μmol/g per min. MVO is myocardial oxygen (atoms) consumption in μmol/g per min estimated from RPP, which is heart rate × mean systolic blood pressure. t is the result of a paired two-tailed t-test comparing low and high work load data. n.s., nonsignificant.

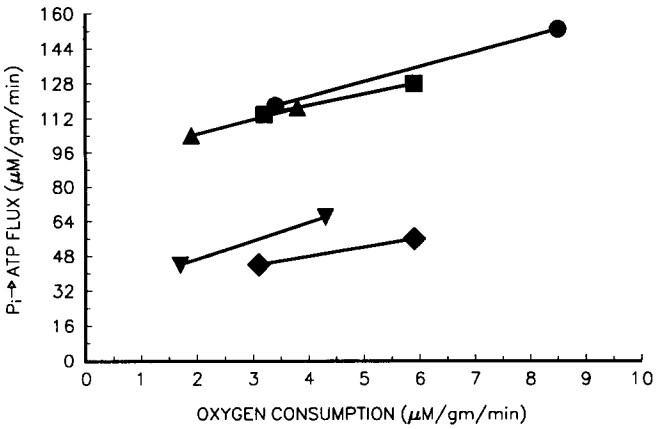

Fig. 4. $P_i \rightarrow$ ATP flux rate (μmol/g per min) is shown versus oxygen consumption (μmol of oxygen atoms/g per min), which is calculated from the rate pressure product. Oxygen consumption is increased through intravenous epinephrine infusion. Each symbol and associated line represent a different animal.

high work load. This finding compares closely to previous estimations of oxygen consumption response using similar epinephrine dosages in this animal model [9,12].

$P_i \rightarrow ATP$ flux

The range of the $P_i \rightarrow$ ATP flux in the low work load state (42–112 μmol/g per min) was extremely broad as shown in Fig. 4. However, the rate of flux increased 16 ± 3 μmol/g per min during epinephrine infusion as calculated myocardial oxygen consumption rate increased by 6.0 ± 0.4 μmol/g per min. In addition to being a consistent finding, paired t test showed that this increase was statistically significant. This change was brought about primarily by significant alterations in M_s/M_0, as τ remains constant. Since longitudinal relaxation (T_1) equals $\tau/M_s/M_0$, then T_1 of P_i spins changes with workload in these experiments. Similarly, Kingsley-Hickman et al have reported that T_1 of the P_i spins in the absence of ATP–P_i exchange varies with workload in perfused hearts [1].

Metabolite stability

10 min spectra (100 acquisitions, interpulse delay 6 s) acquired without selective saturation were available from 3 of the 5 animals. These were obtained both prior to the entire protocol (low work load) and at completion (high work load). The maximum change in calculated P_i concentration between these sets in a single lamb is an 8% decrease and the mean $6\% \pm 1.8$ decrease are similar to the changes between low and high work loads, that are noted in Table 1. These data indicate that P_i/ATP ratio was relatively stable during these protocols.

The analysis of the ATP synthesis rate will be included in discussion.

4. Discussion

Inability to obtain adequate signal to noise and resolution are limitations to performing measurement of $P_i \rightarrow$ ATP flux in vivo. Confirmation that saturation transfer is occurring to intracellular phosphate is the location of the difference spectrum peak at 4.9 ppm as illustrated in Fig. 1C. However, the existence of a small contribution to this difference from other peaks in the same region cannot be totally ruled out. In sheep of the age utilized in this study, blood 2,3-diphosphoglycerate occurs at negligible levels [13]. Therefore, the most likely contamination would occur through inorganic phosphate in the extracellular compartment, including blood in the ventricular chamber. Radiofrequency penetration has been shown to be roughly equivalent to the surface coil radius [15], which was 1.5 cm in these studies. As the left ventricular wall of sheep used in these experiments is > 1.3 cm, and the coil is positioned over the apex where ventricular volume is small, contribution from inorganic phosphate in the ventricular chamber is minimized. Phosphate signal from the remaining extracellular compartment has been shown to be resolvable from the intracellular phosphate using the peak deconvolution program [13], primarily because the extracellular phosphate peak occurs downfield from intracellular phosphate at 5.2–5.3 ppm, depending on blood pH. Limitations in the deconvolution fitting can allow some peak overlap and be a source of error. However, saturation transfer experiments at each work load were obtained during stable conditions. It is extremely unlikely that extracellular phosphate concentrations or the coil's field of view would change during these conditions. Furthermore, saturation transfer from γ ATP to extracellular phosphate would not occur. Then, change in magnetization, M_0–M_s would not be effected by peak contamination or limitations in the deconvolution fitting. These considerations indicate that it is unlikely that contamination of the P_i peak substantially effects the $P_i \rightarrow$ ATP flux measurements performed in these experiments, although this occurrence can not be definitively ruled out.

This study demonstrates the feasibility of measuring $P_i \rightarrow$ ATP flux in myocardium in vivo. However, the $P_i \rightarrow$ ATP flux is not synonymous with the rate of oxidative phosphorylation. Instead, this flux represents the sum of all metabolic transfer of $P_i \rightarrow$ ATP within the system under study [1]. In the case of myocardium, this includes forward ATP synthesis through glycolytic reactions in addition to oxidative phosphorylation. In particular, glyceraldehyde-3-phosphate dehydrogenase and phosphoglycerate kinase have been demonstrated to catalyze their reactions bidirectionally at very high rates [1,2,3]). Since these reactions are bidirectional and possibly exist in a near equilibrium state, then

these $P_i \rightarrow$ ATP flux measurements do not represent net rates. Therefore, the unidirectional rate can be very high, although the net rate may be very low.

In this study, baseline $P_i \rightarrow$ ATP flux was found to average 81 μmol/g per min at an oxygen consumption rate of 5.3 μmol/g per min. If stoichiometrically, approx. 3 mol of ATP are produced per mol of oxygen consumed then only 16 μmol/g per min or less than 24% of this flux can be accounted for by ATP synthesis through oxidative phosphorylation. Thus, the vast majority of $P_i \rightarrow$ ATP flux in normal myocardium in vivo is contributed through glycolytic reactions. The measured $P_i \rightarrow$ ATP flux generated through glycolysis far surpasses the rate that would occur if these reactions operated only in the forward direction. Although net glycolysis could not be measured in this study, this point can be emphasized by assuming that glucose and/or glycogen were the sole substrate for oxidative phosphorylation. Since lactate production in aerobically functioning sheep heart in vivo is negligible [12,18,19], the vast majority of glucose undergoing glycolysis is directed into oxidation. The net rate of glycolysis can then be calculated according to the reaction

$$C_6H_{12}O_6 + 6O_2 \longrightarrow 6CO_2 + 6H_2O$$

by MVO/12, (since oxygen consumption is expressed here as μmol of oxygen atoms/g per min) and equals 0.44 μmol/g per min. If these reactions are considered to be only unidirectional, the forward contribution to $P_i \rightarrow$ ATP flux would be 1.8 μmol/g per min (4 mol ATP produced per mol glucose utilized in glycolysis). Glucose actually supplies less than 20% of the reducing equivalents utilized in oxidative phosphorylation in sheep myocardium [17], so that the forward glycolytic rate is grossly overestimated by this method. Nevertheless, the ${}_{gly}P_i \rightarrow$ ATP flux measured through saturation transfer, approximately 65 μmol/g per min, still exceeds by more than 30-fold the resulting inflated value for glycolytic flux, which is predicted should these reactions function in only the forward direction. These glycolytic reactions then sustain very high bidirectional rates, and therefore exist in a near equilibrium state.

The $P_i \rightarrow$ ATP flux increase, that is associated with an increased rate of oxygen consumption, is a consistent finding in this study. This response is likely due to the raised oxidative phosphorylation rate, and not to altered ${}_{gly}P_i \rightarrow$ ATP flux, which would require a disturbance in the near equilibrium state. Utilizing the data in Fig. 4, the mean $\Delta P_i \rightarrow$ ATP flux/ΔMVO can be calculated by averaging the $\Delta P_i \rightarrow$ ATPflux/ΔMVO changes from the individual experiments. The resultant value, 2.70 ± 0.27 (S.E.) roughly corresponds to the classically accepted P:O value of 3.0 [20–22], although more recent work suggests that a slightly lower value is operative [10]. Studies defining the linear relationship between $P_i \rightarrow$ ATP flux and oxygen consumption during glycolysis elimination in perfused hearts have yielded P:O values between 2.3 and 2.4 [1,2]. The value for $\Delta P_i \rightarrow$ ATP flux/ΔMVO calculated in this study cannot be accepted as a true P:O value without acceding to the assumption that $P_i \rightarrow$ ATP catalyzed by the glycolytic enzymes is constant during this protocol. However, the similarity of this value to generally accepted and experimentally derived P:O values indicates that the change in oxidative phosphorylation is predominantly responsible for the observed increase in $P_i \rightarrow$ ATP flux and that relatively little if any alteration in ${}_{gly}P_i \rightarrow$ ATP flux occurs. A change in the equilibrium position of the glyceraldehyde-3-phosphate dehydrogenase and phosphoglycerate kinase reactions should produce a change in the free cytolsolic ADP concentration with resulting alteration in the PCr/ATP ratio [5]. However, significant changes PCr/ATP do not occur during epinephrine induced oxygen consumption increases in the present animal model under study. Thus, these data do support the contention that the ATP producing glycolytic reactions, glyceraldehyde-3-phosphate dehydrogenase and phosphoglycerate kinase function near equilibrium with minimal disturbance during catecholamine stimulation.

An alternative explanation for the high rate of $P_i \rightarrow$ ATP flux at both work levels is that the enzymes involved in oxidative ATP synthesis such as the translocase and ATP synthase function near equilibrium. The unidirectional $P_i \rightarrow$ ATP flux would then be greater then the net oxidative ATP synthesis rate. However, this theory is less plausible considering findings by LaNoue et al, who showed that the reverse reaction (ATP $\rightarrow P_i$) was far less than the forward $P_i \rightarrow$ ATP flux except at very low oxygen consumption rates in isolated mitochondria [23]. Furthermore, as noted previously, elimination of glycolysis in perfused hearts yields forward $P_i \rightarrow$ ATP flux values which are close to those predicted for the net oxidative phosphorylation rate [1]. Therefore, findings in the above-mentioned studies indicate that the reverse reaction rate must be very low and that the translocase and synthase do not function at or near equilibrium. The stoichiometric relationship estimated from $\Delta P_i \rightarrow$ ATP flux/ΔMVO in the present study also supports this contention.

In summary this study demonstrates the feasibility of measuring $P_i \rightarrow$ ATP flux in myocardium in vivo. These data also provide support for previous studies which suggest that the ATP producing reactions of glycolysis function in a near equilibrium state. The significance of this finding cannot be determined from these experiments. More direct examination of these glycolytic reactions and their regulation in vivo will be required to determine the importance of this near equilibrium state.

Acknowledgements

The technical assistance of Thomas G. Cooper and Deborah Simon is appreciated. This work was funded by Grant R29 HL-47805 awarded by the National Institutes of Health.

References

[1] Kingsley-Hickman, P.B., Sako, E.Y., Mohanakrishnan, P., Robitaille, P.M.L., From, A.H.L., Foker, J.E. and Ugurbil, K. (1987) Biochemistry 26, 7501–7510.
[2] Sako, E.Y., Kingsley-Hickman, P.B., From, A.H.L., Foker, J.E. and Ugurbil, K. (1988) J. Biol. Chem. 263 (22), 10600–10607.
[3] Brindle, K.M. and Radda, G.K. (1987) Biochim. Biophys. Acta 928, 45–55.
[4] Mochizuki, S. and Neely, J.R. (1979) J. Mol. Cell. Cardiol. 11, 221–236.
[5] Neely, J.R., Morgan, H.E. and Owen, P. (1974) Annu. Rev. Physiol. 36, 413–459.
[6] Oguchi, M., Gerth, E., Fitzgerald, B. and Park, J.H. (1973) J. Biol. Chem. 248, 5571–5576.
[7] Opie, L.H., Mansford, K.R.L. and Owen, P. (1971) Biochemistry 124, 475–490
[8] Robitaille, P.M., Merkle, H., Sako, E., Lang, G., Clack, R.M., Bianco, R., From, A.H.L., Foker., J. and Ugurbil, K. (1990) Magn. Res. Med. 15, 8–24.
[9] Portman, M.A., Heineman, F.W. and Balaban, R.S. (1989) J. Clin. Invest. 83, 456–464.
[10] Hsieh, P.S. and Balaban, R.S. (1988) Magn. Res. Med. 7, 56–64.
[11] Katz, L.A., Swain, J.A., Portman, M.A. and Balaban, R.S. (1989) Am. J. Physiol. 256 (Heart Circ. Physiol. 25): H265–H274.
[12] Portman, M.A. and Ning, X.-H. (1992) Am. J. Physiol. 263 (Cell Physiol. 32): C453–460.
[13] Portman, M.A. and Ning, X.-H. (1990) J. Clin. Invest. 86, 1823–1828.
[14] Ingwall, J.S., Kramer, M.F., Woodman, D. and Friedman, W.F. (1981) Pediatr. Res. 15, 1128–1133.
[15] Katz, L.A., Swain, J.A., Portman, M.A. and Balaban, R.S. (1988) Am. J. Physiol. 255 (Heart. Circ. Physiol. 24): H189–H196.
[16] Portman, M.A., Lassen, N.A., Cooper, T.G., Sills, A.M. and Potchen, E.J. (1991) J. Appl. Physiol. 71(6): 2168–2172.
[17] Fisher, D.J., Heyman, M.A. and Rudolph, A.M., (1980) Am. J. Physiol. 234 (Heart. Circ. Physiol. 16): H399–H405.
[18] Drake, A.J., Papadoyannis, D.E., Butcher, R.G., Stubbs, J. and Noble, M.I.M. (1980) Circ. Res. 47(3): 338–345.
[19] Laughlin, M.R., Taylor, J.F., Chesnick, A.S. and Balaban, R.S. (1992) Am. J. Physiol. 262 (Endocrinol. Metabol. 25): E875–E883.
[20] Davis, E.J., Lumeng, L. and Bottoms, D. (1974) FEBS Lett. 39, 9–12.
[21] Hinkle, P.C. and Yu, M.L. (1979) J. Biol. Chem. 254, 2450–2455.
[22] Lenaz, G. and Beyer, R.E. (1965) J. Biol. Chem. 240, 3653–3659.
[23] LaNoue, K.F., Jeffries, F.M.H. and Radda, G.K. (1986) Biochemistry 25, 7667–7675.